A 2D Benchmark for the Verification of the PEBBED Code

International Conference on Reactor Physics, Nuclear Power: A Sustainable Resource

Barry D. Ganapol
Hans D. Gougar
Abderrafi M. Ougouag

September 2008

Idaho National Laboratory

A 2D benchmark for the verification of the PEBBED code

Barry D. Ganapol[a*], Hans D. Gougar[b] and Abderrafi M. Ougouag[b]

[a]*University of Arizona, Tucson, AZ, USA*
[b]*Idaho National Laboratory, Idaho Falls, ID, USA*

Abstract

A new benchmarking concept is presented for verifying the **PEBBED** 3D multigroup finite difference/nodal diffusion code with application to pebble bed modular reactors (PBMRs). The key idea is to perform convergence acceleration, also called extrapolation to zero discretization, of a basic finite difference numerical algorithm to give extremely high accuracy. The method is first demonstrated on a 1D cylindrical shell and then on an r,θ wedge where the order of the second order finite difference scheme is confirmed to four places.

1. Introduction

Recently proposed designs for the pebble bed modular reactor (PBMR) incorporate azimuthally placed control rod banks that require special purpose reactor physics methods for proper analysis. Therefore, appropriate solution standards will be required to ensure that new r,θ z algorithms perform properly and accurately. The intent of this presentation is to provide an algorithm for the establishment of multigroup benchmarks for the 2D-(r,θ) diffusion equation. These benchmarks are to serve as standards of comparison for approximate numerical solution algorithms, such as contained in the **PEBBED** [Terry, 2002] finite difference/nodal diffusion code.

Our approach will be to reformulate a finite difference (FD) scheme to provide extreme accuracy. The FD formulation, often thought to be a crude solution at best, is usually not considered for a benchmark. Its simplicity lacks the elegance of say, a nodal method; however, at the same time its simplicity makes it the most widely used of all numerical solutions algorithms for PDEs. In our proposed solution strategy, we assume finite difference approximations for the two spatial derivative operators of the 2D neutron diffusion equation yielding a multipoint recurrence relation whose number of terms depends on the differencing stencil. We can resolve the recurrence through matrix inversion using banded and/or conjugate gradient solvers. If the differencing scheme is consistent, then by refining the mesh spacing, the solution should become increasingly more accurate. The question arises however, as to just how accurate, since it is virtually impossible to specify accuracy by just one discrete realization. Therefore, a discretization sensitivity study usually accompanies a finite difference formulation to estimate how accurate a solution actually is.--But, can we establish a true benchmark with such a simple FD sensitivity study? The obvious appeal is-- the finite difference formulation is the most basic scheme and therefore the easiest to teach, learn and program. In addition, it represents the notion that simple is best, thus avoiding the complication and expense of higher order schemes.

Corresponding author, ganapol@cowboy.ame.arizona.edu
Tel: 520/621-4728; Fax: 520/621-8191.

2. Multigroup diffusion equation

The fundamental assumptions of the 2D multigroup diffusion equation considered here will not be overly restrictive other than requiring steady state and a heterogeneous medium composed of contiguous homogeneous regions. Each energy group can include fission reactions, with fission neutrons appearing in any group. We allow up- and down- scattering of any stride and each region can have a general space varying fixed source.

The steady state multigroup diffusion equation for homogeneous region k and group g is

$$\left[D_{gk}\nabla^2 - \Sigma_{gk} \right]\phi_{gk}(\boldsymbol{r}) + \chi_g \sum_{g'=1}^{G} \nu\Sigma_{fg'k}\phi_{g'k}(\boldsymbol{r}) +$$

$$+ \sum_{g'=1}^{G} \Sigma_{gg'k}\phi_{g'k}(\boldsymbol{r}) = -Q_{gk}(\boldsymbol{r}) \tag{1}$$

for $0 \le k \le N$, $1 \le g \le G$. We shall specify external boundary conditions as necessary.

In vector form, Eq.(1) in region k, is

$$\boldsymbol{M}_{G,k}(x)\boldsymbol{\phi}_k(x) = -\boldsymbol{q}_k(x) \tag{2a}$$

where

$$\boldsymbol{M}_{Gk}(x) \equiv$$

$$\equiv \begin{bmatrix} \nabla^2 + \gamma_{11,k} & \gamma_{12,k} & \gamma_{13,k} & \cdots & \gamma_{1G,k} \\ \gamma_{21,k} & \nabla^2 + \gamma_{22,k} & \gamma_{23,k} & \cdots & \gamma_{2G,k} \\ \gamma_{31,k} & \gamma_{32,k} & \nabla^2 + \gamma_{33,k} & \cdots & \gamma_{3G,k} \\ \cdots & \cdots & \cdots & \cdots & \cdots \\ \gamma_{G1,k} & \gamma_{G2,k} & \cdots & \cdots & \nabla^2 + \gamma_{GG,k} \end{bmatrix} \tag{2b}$$

and the group flux and source vectors are

$$\boldsymbol{\phi}_k(x) \equiv \begin{bmatrix} \phi_{1k}(x) & \phi_{2k}(x) & \cdots & \phi_{Gk}(x) \end{bmatrix}^T$$

$$\boldsymbol{q}_k(x) \equiv \begin{bmatrix} Q_{1k}(x)/D_{1k} & \cdots & Q_{Gk}(x)/D_{Gk} \end{bmatrix}^T \tag{2c}$$

In Eq.(2b), the nuclear parameters for homogeneous region k are,

$$\gamma_{gg} \equiv \frac{\chi_g \nu\Sigma_{fg} - \left(\Sigma_g - \Sigma_{gg}\right)}{D_g} \tag{2d}$$

$$\gamma_{gg'} \equiv \frac{\chi_g \nu\Sigma_{fg'} + \Sigma_{gg'}}{D_g}, \quad g \ne g'.$$

Equation (2a) now becomes

$$\left[\nabla^2 \boldsymbol{I} + \boldsymbol{\gamma} \right]\boldsymbol{\phi}(\boldsymbol{r}) = -\boldsymbol{q}(\boldsymbol{r}), \tag{3}$$

where we have suppressed the reference to region k.

2.1. Matrix decomposition

A particular simplification of Eq.(3) is possible if we diagonally decompose the interaction matrix $\boldsymbol{\gamma}$ into

$$\boldsymbol{\gamma} = \boldsymbol{T}\boldsymbol{\Lambda}\boldsymbol{T}^{-1},$$

where

$$\boldsymbol{\gamma}\boldsymbol{x} = \lambda\boldsymbol{x},$$

and

$$\boldsymbol{\Lambda} \equiv diag\left\{\lambda_l, l = 1,...,G\right\}$$
$$\boldsymbol{T} \equiv \begin{bmatrix} \boldsymbol{x}_1 & \boldsymbol{x}_2 & \cdots & \boldsymbol{x}_G \end{bmatrix}.$$

By defining

$$\boldsymbol{\Psi}(\boldsymbol{r}) \equiv \boldsymbol{T}^{-1}\boldsymbol{\phi}(\boldsymbol{r})$$
$$S(\boldsymbol{r}) \equiv \boldsymbol{T}^{-1}\boldsymbol{q}(\boldsymbol{r}), \tag{4}$$

we find the following decoupled set of monoenergetic diffusion equations:

$$\left[\nabla^2 + \lambda_k \right]\Psi_k(\boldsymbol{r}) = -S_k(\boldsymbol{r}), \tag{5}$$
$$k = 1, 2, ..., G.$$

Therefore,

$$\boldsymbol{\phi}(\boldsymbol{r}) \equiv \boldsymbol{T}^{-1}\boldsymbol{\Psi}(\boldsymbol{r}). \tag{6}$$

The advantage of this formulation is obvious, since we need only treat the one-group case for each homogeneous region,

$$\left[\nabla^2 + B_s^2\right]\phi(\mathbf{r}) = -q(\mathbf{r}).\qquad(7)$$

3. Finite difference (FD) discretizations

3.1 1D Cylindrical geometry

For this case, Eq.(7) is

$$\left[\frac{1}{r}\frac{d}{dr}r\frac{d\phi(r)}{dr} + B_s^2\right]\phi(r) = -q(r),\quad(8a)$$

with

$$r_0 \le r \le r_n.$$

In the following, we consider only flux boundary conditions

$$\phi(r_0) = \phi_0,\quad \phi(r_n) = \phi_n.\qquad(8b)$$

For a homogeneous medium, the spatial domain $[r_0, r_n]$ is conveniently partitioned into n subintervals each of thickness h_r with $r_{i\pm1/2}$ representing interval centers and h_r given by

$$h_r \equiv \frac{r_n - r_0}{n}.$$

With this convention, the FD approximation to Eqs(8) becomes

$$c_i\phi_{i+1} + b_i\phi_i + a_i\phi_{i-1} = f_i\qquad(9)$$
with

$$c_i \equiv \left[\frac{r_{i+1/2}}{r_i}\right]$$

$$b_i \equiv -\left[\frac{r_{i+1/2} + r_{i-1/2}}{r_i} - h_r^2 B_s^2\right]$$

$$a_i \equiv \left[\frac{r_{i-1/2}}{r_i}\right]$$

$$f_i \equiv -h_r^2 q_i.$$

This approximation provides a test case for the 2D-FD algorithm established next.

3.2. (r,θ)-cylindrical geometry

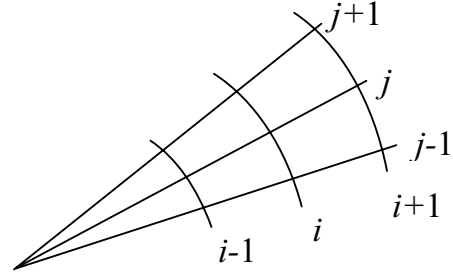We show the specific geometry considered in the following figure:

Fig 1. Homogeneous wedge medium

in which we indicate several homogeneous elements of a heterogeneous wedge. For this geometry, Eq.(7) becomes

$$\left\{\left[\frac{\partial^2}{\partial r^2} + \frac{1}{r}\frac{\partial}{\partial r} + \frac{1}{r^2}\frac{\partial^2}{\partial\theta^2}\right] + B_{s,ij}^2\right\}\phi(r,\theta) = \quad(10)$$
$$= -q(r,\theta)$$

and is discretized in the usual way to give the following FD equation:

$$\alpha_{ij}\phi_{ij} + \beta_i\phi_{i-1,j} + \nu_i\phi_{i+1,j} +$$
$$+ g_i\phi_{i,j-1} + g_i\phi_{i,j+1} = f_{ij}\qquad(11)$$
where

$$\alpha_{ij} \equiv \left[\frac{r_{i+1/2} + r_{i-1/2}}{r_i} + \frac{2}{r_i^2}\left[\frac{h_r}{h_\theta}\right]^2 - h_r^2 B_{s,ij}^2 \right]$$

$$\beta_i \equiv -\left[\frac{r_{i-1/2}}{r_i}\right]$$

$$\nu_i \equiv -\left[\frac{r_{i+1/2}}{r_i}\right]$$

$$g_i \equiv -\frac{1}{r_i^2}\left[\frac{h_r}{h_\theta}\right]^2$$

$$f_{ij} \equiv h_r^2 q_{ij}.$$

A block tridiagonal form for the coefficient matrix then emerges

$$A = \begin{bmatrix} B_1 & C_1 & 0 & ... & & & 0 \\ A_2 & B_2 & C_2 & 0 & ... & & 0 \\ 0 & A_3 & B_3 & C_3 & 0 & ... & 0 \\ ... & & & & & & ... \\ & & & & & & 0 \\ & & & 0 & A_{n-2} & B_{n-2} & C_{n-2} \\ 0 & ... & & & 0 & A_{n-1} & B_{n-1} \end{bmatrix},$$

and we are to solve,

$$A\boldsymbol{\phi} = \boldsymbol{S}$$

for the flux.

4. A 1D benchmark demonstration

It is a numerical fact that the finite difference formulation, as presented above, contains discretization error. One discrete realization therefore cannot guarantee a desired accuracy. Thus, a proper finite difference formulation must include a sensitivity investigation to justify the chosen discretization. Unfortunately, information as to the accuracy of a calculation from an ad-hoc sensitivity study is often inconclusive. Thus, the final discretization chosen can give results far from the truth. For this reason, a consistent sensitivity investigation, leading to benchmark quality results,

is proposed which is nothing less than redefining what a numerical solution to a PDE means.

Consider the points in a discretization space, of (h_i, h_j), to define a discrete map. In essence, the solution (at any i,j), if consistent, corresponding to this realization, is an element in a sequence whose limit, as the discretizations approach zero, approaches the true solution. Thus, the true solution is the limit of a series of discrete realizations rather than just a single one. The key to the limit however is the regularity of the sequence and its rate of convergence. Thus, if we apply convergence acceleration, we could possibly gain numerical advantage.

A particularly efficient convergence acceleration is the Wynn-epsilon (*We*) accelerator [Baker, 1996]

$$\varepsilon_{-1}^{(j)} \equiv 0$$

$$\varepsilon_0^{(j)} \equiv S_j, \quad j = 0,1,...,N$$

$$\varepsilon_{k+1}^{(j)} = \varepsilon_{k-1}^{(j+1)} + \left[\varepsilon_k^{(j+1)} - \varepsilon_k^{(j)}\right]^{-1},$$

$$j = 0,1,...,N-k, \quad k = 0,1,...,N-1$$

where S_j is the sequence of discrete realizations. One interrogates the resulting tableau $\varepsilon_k^{(j)}$ along the diagonal for convergence.

4.1. 1D demonstration of We acceleration

The 1D finite difference (FD) formulation, Eq.(9), will test our proposed benchmarking concept. We assume a 1D homogeneous medium (cylindrical shell) with given fluxes at the inner and outer radii and no external source. For this case, the analytical solution is

$$\phi(r) =$$
$$= \left[\frac{I_0(r_0 k)K_0(rk) - K_0(r_0 k)I_0(rk)}{K_0(r_n k)I_0(r_0 k) - K_0(r_0 k)I_0(r_n k)}\right]\phi_n +$$
$$+ \left[\frac{K_0(r_n k)I_0(rk) - I_0(r_n k)K_0(rk)}{K_0(r_n k)I_0(r_0 k) - K_0(r_0 k)I_0(r_n k)}\right]\phi_0$$

where I_0 and K_0 are modified Bessel functions of the first and second kinds respectively and

$k \equiv \sqrt{|B_s^2|}$ (we assume B_s^2 is negative). N_e uniformly distributed edit points will be interrogated for convergence. By sequentially halving the intervals between edits, a sequence of solutions at the N_e edits will result. Note that the edit points are common to the sequences of all discretizations allowing for their acceleration.

Table 1 gives the error for the highest level discretization (7) for this example where

$$B_s^2 = -1, \ r_0 = 0.5, \ r_n = 2,$$

with boundary conditions

$$\phi_0 = 0, \ \phi_n = 1.$$

On comparing the *We* result to the exact, we observe nearly double precision machine accuracy. Most importantly, the original FD flux is 6 orders of magnitude less accurate. In addition, in comparison to the previous iterate (in columns 3 and 5), the *We* acceleration provides a more realistic assessment of how close the result is to the actual.

We can therefore conclude that the FD formulation wrapped in a *We* acceleration indeed gives benchmark accuracy-- at least for 1D.

4.2. Demonstration of We acceleration: 2D--(r,θ) geometry

The solution of Eq (7) for the (r,θ) wedge shown in Fig. 2 below has been implemented as a FD. i is the index in the r-direction and j in the θ direction. The dimensions of the wedge considered are

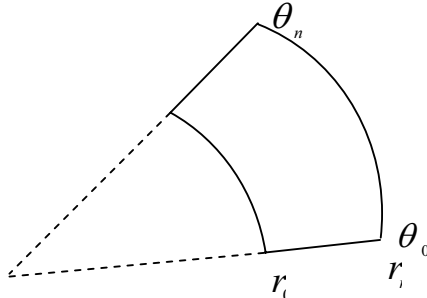$$r_0 = 0.5, \ r_n = 1, \ \theta_0 = 0 deg, \ \theta_n = 20 deg$$

Fig. 2 (r,θ) Single wedge element with $B_s^2 = -1$ and θ-boundary conditions

$$\phi_{0,j} = 0, \ \phi_{n,j} = 0, \ 0 \le j \le n$$
$$\phi_{i,0} = 0, \ \phi_{i,n} = 1, \ 0 \le i \le n.$$

Table 2 shows the last iterate ($l = 6$), where convergence for the accelerated flux is to all places shown. The corresponding original FD iterate has converged to 3-places at best. It would take at least 5 more levels of FD iterations for full convergence of the original FD, which would require more memory than is currently available on planet Earth.

To gain efficiency, we apply the conjugate gradient solver [Park, 2007]. For this, the A-matrix must be symmetric; and the FD scheme of Eqs(11) is not appropriate. The required symmetric form is

$$\alpha_{ij} \equiv \left[\begin{array}{c} r_{i+1/2} + r_{i-1/2} + \dfrac{2}{r_i} \left[\dfrac{h_r}{h_\theta} \right]^2 - \\ -r_i h_r^2 B_{s,ij}^2 \end{array} \right],$$

$$\beta_i \equiv -r_{i-1/2}$$

$$v_i \equiv -r_{i+1/2},$$

$$g_i \equiv -\dfrac{1}{r_i} \left[\dfrac{h_r}{h_\theta} \right]^2,$$

$$f_{ij} \equiv r_i h_r^2 q_{ij}.$$

We find identical results to Table 2 with the CG solver in less than half the computational time.

5. Final confirmation

A general method of generating 2D--(r,θ) multigroup benchmarks for a heterogeneous medium has been proposed and demonstrated on a simple one-node wedge. A sensitive figure of merit of the accelerated solution is the ability to determine the order (2) of the approximation as shown in Table 3. If the exact solution were truly not exact, the order would not be found to the 4-digits displayed.

Table 1
Error for 1D application of *We* at iteration 7

r\error	Original /Original	Original /Exact	We/We	We/Exact
l = 7, *n* = 768				
7.5000E-01	7.31866E-05	2.32143E-07	1.10856E-12	4.97838E-14
1.0000E+00	2.13357E-05	7.65932E-08	4.70085E-13	7.75083E-14
1.2500E+00	2.26140E-06	8.73234E-09	4.55988E-14	8.90054E-14
1.5000E+00	3.95143E-06	1.57704E-08	3.18447E-14	7.74831E-14
1.7500E+00	3.88361E-06	1.55096E-08	1.25654E-13	4.80764E-14

Table 2
(r,θ) 5-Digit Benchmark (θ-Boundary Condition)
l = 6, n = 320

original FD

θ\r	0.6	0.7	0.8	0.9
6.98132E-02	1.32998E-01	1.66577E-01	1.48009E-01	8.81585E-02
1.39626E-01	2.82888E-01	3.44548E-01	3.11058E-01	1.93245E-01
2.09440E-01	4.68885E-01	5.42590E-01	5.03756E-01	3.42759E-01
2.79253E-01	7.09273E-01	7.63220E-01	7.35738E-01	5.92466E-01

accelerated

6.98132E-02	1.32999E-01	1.66579E-01	1.48010E-01	8.81581E-02
1.39626E-01	2.82892E-01	3.44551E-01	3.11060E-01	1.93245E-01
2.09440E-01	4.68893E-01	5.42594E-01	5.03758E-01	3.42758E-01
2.79253E-01	7.09285E-01	7.63223E-01	7.35740E-01	5.92472E-01

Table 3
Confirmation of the approximation order using the
We Accelerator

6.98132E-02	2.0002E+00	2.0000E+00	1.9999E+00	1.9999E+00
1.39626E-01	1.9999E+00	1.9999E+00	2.0000E+00	2.0000E+00
2.09440E-01	2.0000E+00	2.0000E+00	2.0000E+00	2.0000E+00
2.79253E-01	2.0000E+00	1.9999E+00	1.9994E+00	1.9997E+00

References

Terry, W. K., H. D. Gougar, and A. M. Ougouag, "Direct Deterministic Method for Neutronics Analysis and Computation of Asymptotic Burnup Distribution in a Recirculating Pebble-Bed Reactor," Annals of Nuclear Energy **29** (2002) 1345 –1364.

Baker, G and P. Graves-Morris (1996), *Pade' Approximants* (Cambridge University Press, NY).

Park ,R., Private communication, INL, May, 2007.